

H₃-Receptor Antagonists: Synthesis and Structure–Activity Relationships of Para- and Meta-Substituted 4(5)-Phenyl-2-[[2-[4(5)-imidazolyl]ethyl]thio]imidazoles

Marco Mor,[†] Fabrizio Bordi,[†] Claudia Silva,[†] Silvia Rivara,[†] Patrizia Crivori,[†] Pier Vincenzo Plazzi,^{*,†} Vigilio Ballabeni,[‡] Antonio Caretta,[‡] Elisabetta Barocelli,[‡] Mariannina Impicciatore,[‡] Pierre-Alain Carrupt,[§] and Bernard Testa[§]

Dipartimento Farmaceutico and Istituto di Farmacologia e Farmacognosia, Università degli Studi di Parma, Viale delle Scienze, I-43100 Parma, Italy, and Institut de Chimie Thérapeutique, Université de Lausanne, CH-1015 Lausanne, Switzerland

Received February 4, 1997[Ⓢ]

We report the synthesis, octanol/water partition coefficient ($\log P$), dissociation constants (pK_a), H₃-receptor affinity (pK_i in rat brain membranes, [³H]-N^ε-methylhistamine), and H₃-antagonist potency (pA_2 in guinea ileum, (*R*)- α -methylhistamine) of novel H₃-receptor antagonists obtained by introducing a para or meta substituent on the phenyl ring of the lead compound 4(5)-phenyl-2-[[2-[4(5)-imidazolyl]ethyl]thio]imidazole (**3a**). The substituents were chosen to obtain broad and uncorrelated variation in their lipophilic, electronic, and steric properties. The $\log P$ values of the neutral species cover almost 3 orders of magnitude (from 1.40 to 4.11). The $pK_{a,2}$ values (protonation of the 2-thioimidazole fragment) vary from 3.13 to 4.34, indicating that this fragment, which incorporates the so-called polar group common to many H₃-receptor antagonists, is neutral at physiological pH. The compounds had pK_i values in a range too narrow (from 7.28 to 8.03) to derive QSAR equations. In one case (**3g**), a biphasic displacement curve was observed ($pK_{i,1} = 8.53$; $pK_{i,2} = 6.90$). The pA_2 values ranged 2 orders of magnitude (from 6.83 to 8.87) and yielded a QSAR model (PLS) indicating that antagonist potency depends parabolically on lipophilicity and is decreased by bulky para substituents. The compounds of this series, therefore, maintain a fair-to-good affinity for rat brain H₃-receptor and a fair-to-good H₃-antagonist potency on guinea pig ileum, although varying markedly in their lipophilicity. The series thus appears as a good candidate for pharmacokinetic optimization leading to brain-penetrating H₃-receptor antagonists.

Introduction

The histamine H₃-receptor is a G-protein-coupled receptor which controls the synthesis and release of histamine, and the release of other neurotransmitters, from nerve endings.^{1,2} H₃-receptor antagonists inhibit the action of the physiological agonist, thus enhancing neurotransmission. The increase in histaminergic and cholinergic³ transmission in the CNS suggests potential therapeutic uses of brain-penetrating H₃-receptor antagonists in a number of diseases such as epilepsy,^{4,5} vertigo,⁶ cognitive disorders,^{7,8} and obesity.⁹

Different classes of H₃-receptor antagonists have been reported,^{10–12} comprising some high-potency agents such as the lead compounds thioperamide,¹³ clobenpropit,¹⁴ iodophenpropit,¹⁵ and iodoproxyfan.¹⁶ With respect to thioperamide and clobenpropit, an attempt was made to replace the potentially toxic thiourea and isothiurea groups with bioisosteric moieties and even heterocycles.^{17–19} Another aim in the design of H₃-receptor antagonists has been easy access to the CNS, which can be retarded by protonation, as in clobenpropit, or by other distribution phenomena such as the high binding to plasma proteins, as observed for thioperamide.²⁰

From a structural point of view, H₃-receptor antagonists are characterized by the presence of an imidazole ring connected by an alkyl spacer to a polar group, which in turn is attached to a lipophilic ending group. One possible classification of these compounds considers the polar group, which can be strongly basic and thus protonated at physiological pH (e.g. clobenpropit), or neutral as in thioperamide. The state of protonation can affect not only the pharmacokinetic behavior of the drug, but also the structure–activity profile of a series of analogs. The basicity of the polar group is therefore a crucial feature in the study of structure–activity relationships for H₃-receptor antagonists. Furthermore, given the importance of the lipophilic ending group in many classes of H₃-receptor antagonists, it is also of interest to investigate the effect of lipophilicity on receptor affinity and antagonist potency.

Our studies on H₃-receptor antagonists began with the inclusion of the carbothioamide fragment of thioperamide in a benzo-condensed heterocycle, giving a series of 1-(benzothiazol-2-yl)-4-[4(5)-imidazolyl]piperidine derivatives.^{21,22} A QSAR study in this series suggested the need for less bulky or more flexible structures to achieve higher H₃-receptor affinities. A series of [(heteroaryl)amino]ethyl- and [(heteroarylthio)ethyl]imidazoles was therefore synthesized and tested,^{18,23} with the polar group represented by an imidazole or thiazole ring or by their benzo-condensed derivatives. Among the most promising compounds, the (4-phenyl-2-imidazolyl)thio derivative (**3a** in Table 1) showed good affinity for central H₃-receptors ($pK_i = 7.85 \pm 0.06$) and

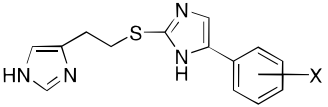
* To whom correspondence should be addressed. Fax: +39 521 905006. E-mail chifar@ipruniv.cce.unipr.it.

[†] Dipartimento Farmaceutico, Università degli Studi di Parma.

[‡] Istituto di Farmacologia e Farmacognosia, Università degli Studi di Parma.

[§] Université de Lausanne.

[Ⓢ] Abstract published in *Advance ACS Abstracts*, July 1, 1997.

Table 1. Histamine H₃-Receptor Affinity and Antagonist Potency of Compounds **3a–l**


compd	X	p <i>K</i> _i ^a	p <i>A</i> ₂ ^b
3a	H	7.85 ± 0.06	8.19 ± 0.18
3b	<i>p</i> -Cl	7.45 ± 0.04	8.87 ± 0.18
3c	<i>p</i> -NO ₂	7.28 ± 0.04	7.79 ± 0.25
3d	<i>p</i> - <i>O</i> - <i>n</i> -C ₄ H ₉	7.71 ± 0.06	6.83 ± 0.09
3e	<i>p</i> - <i>n</i> -C ₃ H ₇	7.40 ± 0.08	— ^c
3f	<i>p</i> -N(CH ₃) ₂	7.53 ± 0.05	7.28 ± 0.09
3g	<i>p</i> -OSO ₂ C ₆ H ₅	8.53 ± 0.20 ^d	7.30 ± 0.04
3h	<i>p</i> -CONH ₂	6.90 ± 0.42 ^d	6.93 ± 0.12
3i	<i>m</i> -Br	7.55 ± 0.03	8.11 ± 0.29
3j	<i>m</i> -NO ₂	7.85 ± 0.04	8.46 ± 0.18
3k	<i>m</i> - <i>O</i> - <i>n</i> -C ₃ H ₇	7.51 ± 0.03	— ^c
3l	<i>m</i> -CONH ₂	8.03 ± 0.02	6.84 ± 0.13
		7.79 ± 0.04	

^a Inhibition of [³H]NAMHA binding to rat brain membranes.

^b H₃-antagonist potency on electrically stimulated guinea pig ileum.

^c Unsurmountable antagonism at concentration > 10⁻⁷ M.

^d A two-site model gave a significantly better fit. The relative proportions of the high (p*K*_{i,1}) and low (p*K*_{i,2}) affinity site were 66% and 34%, respectively.

good H₃-receptor antagonist potency on electrically stimulated guinea pig ileum (p*A*₂ = 8.19 ± 0.18). Compound **3a** was therefore taken as a putative lead compound in the subsequent optimization study described here.

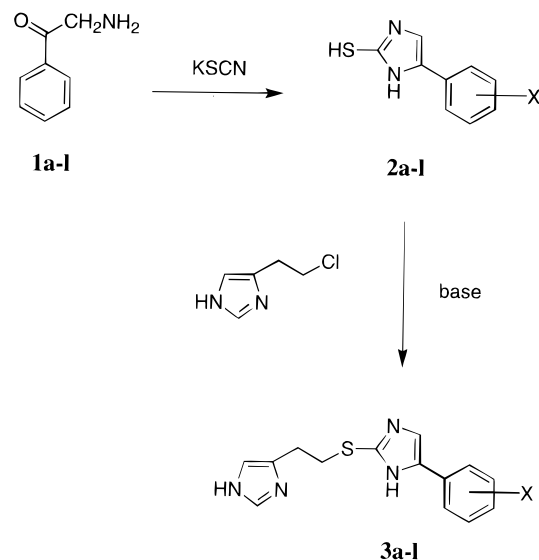
In the present work, we have modulated the physicochemical features of the terminal group, introducing meta or para substituents on the phenyl ring of compound **3a**, with the aim of assessing their influence on lipophilicity and ionization and exploring their effect on H₃-receptor antagonist potency and affinity. Here, we report the synthesis, physicochemical parameters (log *P* and p*K*_a values measured by the pH-metric method²⁴), binding affinity to rat brain H₃-receptor, H₃-receptor antagonist potency on electrically stimulated guinea pig ileum, and structure–activity relationships of compounds **3a–l**. In order to establish the H₃ selectivity of these new compounds, we tested them on H₁- and H₂-receptors as well.

Design

The substituents were chosen to obtain broad, uncorrelated variations in their lipophilic, electronic, and steric properties. They were introduced in the para or meta position, avoiding ortho substitution which could lead to unpredictable conformational effects. For both para and meta substituents, the selection was made starting from a factorial design, which proved biased due to uneven distribution in the parameter space and to the criterion of good synthetic accessibility. The compounds were therefore selected by considering the D-efficiency²⁵ of the overall design.

The variable space was defined by the physicochemical parameters π , σ , and MR for the 100 aromatic substituents reported by Skagerberg *et al.*²⁶ In the case of para substituents, an initial two-level full factorial design²⁷ led to the selection of eight substituents, some of which were replaced by others considered more accessible from a synthetic point of view. The replacements were carried out with the aid of the D-optimal design program DESDOP.²⁸ In particular, the substitu-

Scheme 1



ent CONH₂ belongs to the same octant as NO₂ (that of the hydrophilic, electron-withdrawing small substituents), but its inclusion allowed the reduction of the correlation coefficient between π and MR from 0.57 to 0.48, and it increased the lipophilicity range by more than 1 unit. The final D-efficiency for the eight para substituents was 42.8%, starting from the entire set of 100 substituents. Ranges of variables for para substituents were as follows: π , -1.49 (CONH₂) to 1.55 (*O*-*n*-C₄H₉); σ , -0.83 (N(CH₃)₂) to 0.78 (NO₂); MR, 1.03 (H) to 36.7 (OSO₂C₆H₅). Correlation coefficients were as follows: π - σ , -0.29; π -MR, 0.48; σ -MR, 0.03.

For meta substitution a simpler design was applied: four substituents (H, NO₂, *O*-*n*-C₃H₇, Br) were selected according to a factorial design on π and σ , and a further substituent (CONH₂) was added as proposed by DESDOP, in order to expand the range of lipophilicity and to obtain a low correlation between π and the steric descriptor MR. For meta substituents, ranges were as follows: π , -1.49 (CONH₂) to 1.05 (*O*-*n*-C₃H₇); σ , 0.00 (H) to 0.71 (NO₂); MR, 1.03 (H) to 17.1 (*O*-*n*-C₃H₇). Correlation coefficients were as follows: π - σ , -0.19; π -MR, 0.33; σ -MR, 0.01.

Chemistry

For the synthesis of the desired compounds (Table 1), a general and simple synthetic route was employed, starting from easily accessible acetophenone derivatives. The compounds were prepared (Scheme 1) starting from phenyl-substituted ω -aminoacetophenones (**1a–l**), which were synthesized by a Delepine reaction starting from commercially available ω -bromoacetophenones. The phenyl-substituted ω -aminoacetophenones (**1a–l**) were cyclized with potassium thiocyanate to 4(5)-(X-phenyl)-2-mercaptoimidazoles (**2a–l**). These were then condensed with 4(5)-(2-chloroethyl)imidazole, employing appropriate acceptor bases and experimental conditions (see Experimental Section), giving the desired products **3a–l**. For the two carbamoyl derivatives, **3h** and **3l**, the intermediates **2h** and **2l** were prepared with a cyano group on the phenyl ring; the CN group was then hydrolyzed to a CONH₂ group before condensation with (chloroethyl)imidazole.

Pharmacology

The H₃-receptor affinity was determined by the displacement of [³H]-N^α-methylhistamine bound to rat cerebral cortex membranes, whereas the H₃ antagonist potency was assessed by the inhibition of (*R*)-α-methylhistamine-induced responses on the electrically stimulated guinea pig ileum. Possible interactions at H₁- and H₂-receptor subtypes were investigated on histamine-induced contractions of the guinea pig isolated ileum and on dimaprit-evoked chronotropic responses of guinea pig isolated atria, respectively.

Results and Discussion

log P(BH⁺), log P(B), and pK_a. The results of pK_a and log P determinations are reported in Table 2. The low stability of compound **3f** (X = N(CH₃)₂) made its study impossible. The two dissociation constants refer to the two imidazole rings, the lower (pK_{a,1}) and higher (pK_{a,2}) values corresponding respectively to the 4(5)-phenyl-2-thioimidazole and 4(5)-alkylimidazole moieties. Two values of log P are also reported, one for the monoprotonated species (log P(BH⁺)) and the second for the free base (log P(B)). A high variation in lipophilicity was produced by the substituents, since log P(B) varies from 1.4 (**3h**) to 4.11 (**3d**). This is in good agreement with the π values of the substituents (eq 1).

$$\log P(B) = 0.885(\pm 0.045)\pi + 2.83(\pm 0.05) \quad (1)$$

$$n = 11; \quad r^2 = 0.977; \quad s = 0.155; \quad F = 383.5$$

The protonation of the stronger basic center produces a decrease in log P of about 2.7 units [log P(B) - log P(BH⁺) = 2.69 ± 0.23]. Thus, whereas the free bases are relatively lipophilic and have a good potential for brain penetration, protonation leads to intrinsically hydrophilic species which as such have a low potential for passive diffusion into the brain. The first protonation is believed to occur at the 4(5)-alkylimidazole ring, as the values of the higher dissociation constant (pK_{a,2}) are quite constant around 7, similar to the pK_a of free imidazole. The pK_{a,1} values reflect the inductive effect of the sulfur atom in position 2 and the electronic effect of the substituents in position 4(5) of the second imidazole ring. The variation in pK_{a,1} can in fact be correlated with the σ values of aromatic substituents²⁶ (eq 2).

$$pK_{a,1} = -1.17(\pm 0.15)\sigma + 4.18(\pm 0.06) \quad (2)$$

$$n = 11; \quad r^2 = 0.865; \quad s = 0.161; \quad F = 57.9$$

The separation of inductive and resonance effects, as described by *F* and *R*,²⁹ did not bring about any significant improvement in the correlation with pK_{a,1} (eq 3).

$$pK_{a,1} = -1.41(\pm 0.24)F - 0.943(\pm 0.249)R + 4.27(\pm 0.10) \quad (3)$$

$$n = 11; \quad r^2 = 0.885; \quad s = 0.157; \quad F = 30.9$$

As a result of these various contributions, the so-called polar group of this series has a markedly reduced basicity (pK_{a,1} range: 3.13–4.34) and will be uncharged at physiological pH. The present compounds can there-

Table 2. Dissociation Constants and Partition Coefficients of Compounds **3a–l**

compd	pK _{a,1} ^a	pK _{a,2} ^b	log P(BH ⁺) ^c	log P(B) ^d
3a	4.28	7.07	-0.15	2.62
3b	4.12	7.10	1.02	3.66
3c	3.13	6.94	0.00	2.75
3d	4.30	7.06	1.21	4.11
3e	4.34	7.03	1.36	4.09
3f^e				
3g	3.84	6.93	0.81	3.72
3h	3.63	7.07	-1.34	1.4
3i	3.90	7.08	0.94	3.76
3j	3.21	6.89	-0.13	2.43
3k	4.04	7.04	0.99	3.7
3l	4.01	7.05	-0.46	1.61

^a Basicity of the substituted imidazole ring. ^b Basicity of the unsubstituted imidazole ring. ^c log P of monocation. ^d log P of neutral species. ^e The compound was not stable enough.

fore be classified as thioperamide-like H₃-receptor antagonists, characterized by neutral polar groups.

H₃-Receptor Binding Affinity and Antagonist Potency. Table 1 reports the pK_i values of compounds **3a–l** as measured in rat brain cortex preparations. Comparable affinities were observed for all compounds in the series (pK_i range 7.28–8.03). Compound **3g** (the (*p*-phenylsulfonyl)oxy derivative) showed a slightly biphasic curve in its inhibition of [³H]-N^α-methylhistamine binding ([³H]NAMHA), yielding a significantly better fit with a two-site model (pK_{i,1} = 8.53, pK_{i,2} = 6.90) with relative proportions of 66% and 34%, respectively. A biphasic inhibition curve had been observed also for thioperamide,³⁰ but the presence of sodium ions in the buffer rendered the curve monophasic. This is the first time that a biphasic curve is reported for an H₃-receptor antagonist displacing [³H]NAMHA in the presence of 50 mM NaCl. Such biphasic curves can be due to receptor heterogeneity or to the presence of different conformations/states of the same receptor.³⁰

In the functional studies, all of the compounds tested (except **3e** and **3k**) competitively antagonized (*R*)-α-methylhistamine-induced responses, showing different potencies as indicated by the pA₂ values reported in Table 1. Above 10⁻⁷ M, *p*-propyl- (**3e**) and *m*-propoxy- (**3k**) substituted compounds displayed an unsurmountable antagonism, shifting rightward the H₃-receptor antagonist concentration–response curve and simultaneously reducing its maximum. Within this series, the highest H₃-antagonist potency was that of compound **3b**, which showed an increase of 0.68 in pA₂ value relative to the parent compound (**3a**).

Some differences are evident between the binding and functional data, namely a larger variation in pA₂ than in pK_i values, and a different ranking order. Thus, compound **3b** (*p*-Cl) was the most potent antagonist but did not have the highest affinity. Compound **3k** (*m*-O-*n*-C₃H₇) had the highest affinity but displayed a non-competitive behavior in the functional test. Moreover, compounds **3d**, **3h**, and **3l** had a significantly lower potency than the other compounds in the functional test, but their affinity was similar to that of the parent compound. Relevant differences between binding affinities in rat brain cortex and potencies in guinea pig ileum have been reported for H₃-receptor antagonists,^{31–33} but it is still unclear whether this can be attributed to receptor heterogeneity, nor are structural features known that could discriminate between these activities.

Table 3. Partial Weights of the Two Latent Variables (LV) and Pseudocoefficients of Physicochemical Variables vs pA_2 Obtained for the PLS Model

no.	variable	partial weights		pseudo-coefficients ^a
		1st LV	2nd LV	
1	π^b	0.1795	0.5886	0.2382
2	π^2	-0.5378	-0.3975	-0.3533
3	σ^b	0.2571	-0.0425	0.2195
4	F ^c	0.2638	0.1108	0.7336
5	R ^c	excluded	excluded	
6	MR $p^{b,d}$	-0.3374	0.2595	-0.0071
7	L $p^{d,e}$	-0.3292	0.2983	-0.0321
8	B $_1p^{d,e}$	excluded	excluded	
9	B $_5p^{d,e}$	-0.4387	0.1504	-0.1177
10	S $_bp^{d,f}$	-0.3563	0.1919	-0.0594
11	MR $m^{b,g}$	excluded	excluded	
12	L $m^{e,g}$	0.0342	-0.5154	-0.1465
13	B $_1m^{e,g}$	excluded	excluded	
14	B $_5m^{e,g}$	excluded	excluded	
15	S $_bm^{f,g}$	excluded	excluded	
intercept				8.62

^a Referred to original unscaled variables. ^b Taken from Skagerberg *et al.*²⁶ ^c Taken from Skagerberg *et al.*²⁶ for meta substituents; F and R were weighted by the positional weighting factors $f_{\text{meta}} = 0.980$ and $r_{\text{meta}} = 0.347$ (see ref 34). ^d p indicates para substituents. ^e Taken from Hansch *et al.*²⁹ ^f Branching parameter from Austel *et al.*³⁵ ^g m indicates meta substituents.

H₁- and H₂-Receptor Activity. The compounds tested did not exhibit any remarkable inhibition of H₁ and H₂ mediated responses up to 10⁻⁶ M.

QSAR. No QSAR study was undertaken for the binding data (pK_i), given the small variation in affinity over the entire set of ligands. Indeed, excluding compound **3g** which had a biphasic inhibition curve, the standard deviation of the average pK_i was 0.247. Thus structural variations on the phenyl ring did not influence markedly receptor affinity, despite the broad exploration of parameter space achieved with the selected substituents.

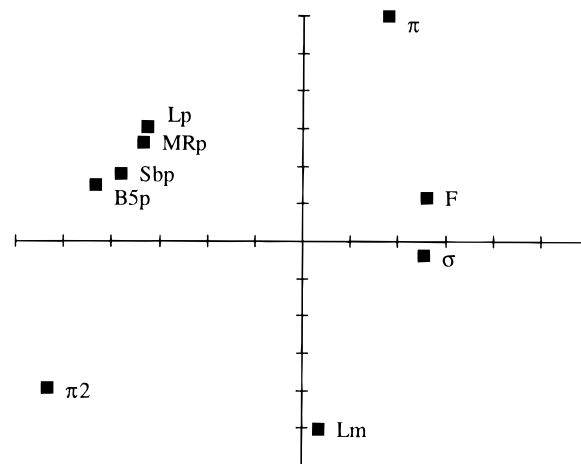
Much larger variations were seen in the pA_2 data. Two compounds (**3e** and **3k**) did not yield potency data consistent with the other pA_2 since they showed non-competitive antagonism with unsurmountable decrease in the maximum effect of the agonist (*R*)- α -methylhistamine at concentrations > 10⁻⁷ M. For the 10 remaining compounds, no simple quantitative relation between pA_2 and log *P* or $pK_{a,1}$ was obtained. A decrease in potency at the two extremes of the lipophilicity range (compounds **3d**, **3h**, and **3l**) was observed, whereas variation in the basicity of the polar group ($pK_{a,1}$) was not sufficient to cause effective differences in protonation at physiological pH and to influence *in vitro* potency.

Since the lack of simple correlations could be due to complex structure-activity relationships, we investigated the correlation between pA_2 and a multivariate description of physicochemical properties. Fifteen variables were used, taken from different literature sources and describing the lipophilic, electronic, and steric properties of the substituents (Table 3). In this multivariate characterization, the π values were used instead of experimental log *P* values, since they were highly correlated with experimental lipophilicity (eq 1), and it was not possible to measure the log *P* of compound **3f**. The square of the lipophilicity parameter (π^2) was included to account for a second-degree effect in the low potency of highly hydrophilic and lipophilic substituents. The field and resonance descriptors (F and R) were

Table 4. Observed and Calculated pA_2 Values^a

compd	substituent	pA_2	
		obsd	calcd
3a	H	8.19	8.12
3b	<i>p</i> -Cl	8.87	8.23
3c	<i>p</i> -NO ₂	7.79	8.24
3d	<i>p</i> -OC ₄ H ₉	6.83	6.86
3f	<i>p</i> -NMe ₂	7.28	7.51
3g	<i>p</i> -OSO ₂ Ph	7.30	7.31
3h	<i>p</i> -CONH ₂	6.93	6.71
3i	<i>m</i> -Br	8.11	8.22
3j	<i>m</i> -NO ₂	8.46	8.45
3l	<i>m</i> -CONH ₂	6.84	6.94

^a The latter were obtained with the PLS model whose partial weights are reported in Table 3.

**Figure 1.** Partial weights of the descriptors in the first two latent variables (LV) of the PLS model. The first LV is represented in the abscissa.

weighted according to Norrington *et al.*³⁴ for meta substituents. The steric parameters, comprising bulkiness (MR), shape (L, B₁, and B₅), and a topological descriptor (S_b),³⁵ were split for para and meta substitution.

Multiple linear regression analysis (MRA) was not an appropriate tool in this study, given the high risk of chance correlations with variable selection.³⁶ A PLS analysis with the 15 descriptors listed in Table 3 was therefore performed, controlling the number of latent variables by cross-validation. By using all the 15 variables, the best Q^2 (0.42, SDEP = 0.53) was obtained for the two-latent-variables model, which had an $r^2 = 0.84$ (SDEC = 0.27). The variable selection implemented in GOLPE^{37,38} allowed discrimination between informative and noisy descriptors, and actually the exclusion of variables 5 (R), 8 (B₁p), 11 (MR m), 13 (B₁m), 14 (B₅m), and 15 (S_bm) gave a PLS model with the same descriptive capacity ($r^2 = 0.84$, SDEC = 0.27) and a significantly better predictive power ($Q^2 = 0.63$, SDEP = 0.42). The characteristic data of this model are reported in Tables 3 and 4 and represented in Figures 1 and 2. As seen in Figure 1, the first latent variable (LV) is related mainly to the dimension of the para substituents and to π^2 , both with negative weights, while the highest absolute values for the second LV are presented by lipophilicity (positive), its squared value (negative), and the length of the meta substituents. The contribution of the electronic parameters is lower. This is confirmed by the fact that excluding those parameters, whose influence on the predictive power was considered

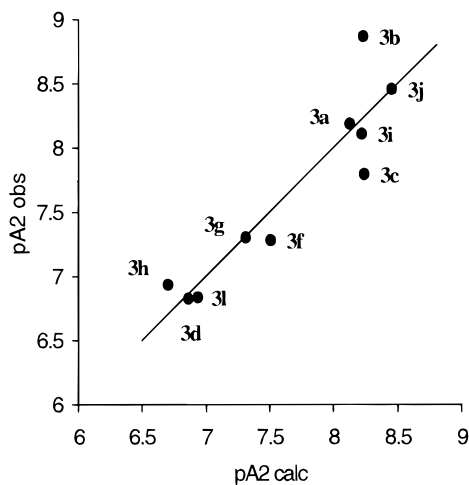


Figure 2. The relation between observed pA_2 values and those calculated with the best PLS model.

as uncertain by the GOLPE³⁸ procedure, gave a model with $r^2 = 0.74$ and $Q^2 = 0.44$ (2 LV) based only on variables 1 (π), 2 (π^2), and 9 (B_5p). These three variables therefore contain sufficient information to explain most of the pA_2 variation accounted for by the model with nine variables.

A broad parabolic dependence on lipophilicity and a negative effect of steric hindrance in the para position are the main relations that emerge between physicochemical descriptors and antagonist potency. The low significance of steric parameters for meta substituents is probably caused by loss of information due to the exclusion of compound **3k** (which has the bulkiest meta substituent).

The relation between observed pA_2 values and those calculated with the best PLS model is shown in Figure 2. As can be seen, the PLS model can only discriminate between two groups of compounds having low (**3d**, **3f**, **3g**, **3h**, and **3l**) or medium-to-high potencies (**3a**, **3b**, **3c**, **3i**, and **3j**). This feature is common to all the PLS models employed here independently of variable exclusion and can be ascribed to experimental uncertainty in pA_2 determination or to loss of information in structure parametrization. The model described is insufficient to make new predictions, particularly for meta substitution, where the noncompetitive antagonism of compound **3k** results in loss of information. However, the model can suggest an explanation for the differences observed between pA_2 and pK_i values.

Indeed, the model shows that an optimal lipophilicity range (around $\pi = 0.34$) is required for high pA_2 , as calculated from PLS pseudocoeficients (see Table 3). This optimal range is not observed with affinity data, perhaps reflecting a different access to the active site in the two tests. The negative steric effect of para substituents, observed only in pA_2 , is difficult to explain unless highly hypothetical differences in the topography of the two binding sites are evoked.

Conclusion

The *m*- and *p*-phenyl derivatives of 4(5)-phenyl-2-[[2-[4(5)-imidazolyl]ethyl]thio]imidazole (**3a**) represent a new class of antagonists with good affinity for rat brain H₃ binding sites and with interesting selectivity and potency for the guinea pig ileum H₃-receptor. These agents have an imidazole ring that acts as the polar

group in the general formula of the H₃-receptor antagonists. Because this imidazole ring is not protonated at physiological pH, this class of compounds belongs to the thioperamide-like group of H₃-receptor antagonists.

With the introduction of substituents on the phenyl ring, the lipophilicity of the uncharged species spans a wide range of log *P* values around 2, while there is relatively little variation in receptor affinities. This characteristic could be gainfully exploited to optimize pharmacokinetic properties such as protein binding and brain penetration.

The H₃-receptor antagonist potency in the guinea pig ileum follows a different structure–activity pattern than the affinity for rat brain H₃-receptors. Indeed, the dependence of this activity on physicochemical properties is more apparent, an optimal lipophilicity range and a reduced steric hindrance in the para position representing crucial requirements to provide high H₃ antagonist potency. Such differences could perhaps be due to receptor heterogeneity or to different access to the active site.

The H₃-receptor antagonists presented here are therefore of potential interest due to their good affinity and potency, and to their relative tolerance to physicochemical modulation aimed at pharmacokinetic optimization.

Experimental Section

Chemistry. Melting points (uncorrected) were measured with a Büchi instrument (Tottoli). The newly synthesized compounds were analyzed for C, H, and N. The ¹H-NMR spectra were recorded on a Bruker 300 spectrometer (300 MHz) with tetramethylsilane (TMS) as the internal standard. Samples were dissolved in DMSO-*d*₆, unless indicated otherwise.

Reactions were monitored by TLC on Kieselgel 60 F 254 (DC-Alufolien, Merck). The products of the reactions were controlled by IR and mass spectroscopy. Compounds and intermediates were purified by chromatography on a preparative Gilson HPLC using an SiO₂ column (LiChroprep., Si60, 15–25 μ m, Merck); the eluents were mixtures of CH₂Cl₂/MeOH or CHCl₃/MeOH at various volume ratios.

General Method of Preparation of Substituted 4(5)-Phenyl-2-mercaptoimidazole Derivatives (2a–l). Substituted 4(5)-phenyl-2-mercaptoimidazole derivatives (Scheme 1: **2a**,¹⁸ **2b**,³⁹ **2c–g**, and **2i–k**) were prepared from the corresponding ω -aminoacetophenones and KSCN following the general method of Norris³⁹ (in CH₃COOH) or that of Pyman⁴⁰ (in water). For *p*- and *m*-carbamoyl derivatives (**2h** and **2l**), the cyclization was performed from *p*- and *m*-cyano- ω -aminoacetophenone, giving 4(5)-(4-cyanophenyl)-2-mercaptoimidazole and 4(5)-(3-cyanophenyl)-2-mercaptoimidazole, respectively; these were then hydrolyzed to the respective carbamoyl derivatives by addition of water, according to the method of Snyder.⁴¹

Yields and melting points of the newly synthesized intermediates were as follows: **2c** (X = *p*-NO₂) yield 40%, mp 278–279 °C dec; **2d** (*p*-O-*n*-C₄H₉) yield 45%, mp 230 °C; **2e** (*p*-*n*-C₃H₇) yield 40%, mp 250–253 °C dec; **2f** (*p*-N(CH₃)₂) yield 31%, mp 229–231 °C; **2g** (*p*-OSO₂C₆H₅) yield 31%, mp 237–239 °C; **2h** (*p*-CONH₂) yield 90%, mp 302–303 °C; **2i** (*m*-Br) yield 67%, mp 272.5–274 °C; **2j** (*m*-NO₂) yield 40%, mp 283–285 °C dec; **2k** (*m*-O-*n*-C₃H₇) yield 45%, mp 250–253 °C dec; **2l** (*m*-CONH₂) yield 75%, mp 299–302 °C.

General Method of Condensation of 2-Mercaptoimidazole Derivatives with 4(5)-(2-Chloroethyl)imidazole (Preparation of Compounds 3a–l). Compounds **3a–l** were prepared, according to Scheme 1, starting from 4(5)-(2-chloroethyl)imidazole and the appropriate mercaptoheterocycle as a nucleophile, in the presence of EtONa in DMSO at room temperature. Equimolar ratios of (chloroethyl)imidazole/nucleophile were used, with double molar ratio of base, because

(chloroethyl)imidazole hydrochloride was employed as the starting compound. Reactions were followed by TLC (SiO₂, CH₃COOEt/EtOH/NH₃(aq) 6/1/1); at the end of the reaction (1–48 h) the products were precipitated with water, purified by column chromatography, and crystallized, generally as dihydrochlorides.

4(5)-(Phenyl)-2-[[2-[4(5)-imidazolyl]ethyl]thio]imidazole dihydrochloride (3a·2HCl): yield 65%; mp 243–246 °C from propanol; ¹H-NMR (DMSO-*d*₆) δ 3.07 (t, *J* = 7.0 Hz, 2H, CH₂), 3.70 (t, *J* = 7.0 Hz, 2H, CH₂-S), 7.39 (t, *J* = 7.4 Hz, 1H, Ph-4-H), 7.48 (t, *J* = 7.4 Hz, 2H, Ph-3-H), 7.57 (s, 1H, Im-5-H), 7.92 (d, *J* = 7.4 Hz, 2H, Ph-2-H), 8.15 (s, 1H, Ph-Im-5-H), 9.03 (s, 1H, Im-2-H). Anal. (C₁₄H₁₄N₄S·2HCl) C, H, N.

4(5)-(4-Chlorophenyl)-2-[[2-[4(5)-imidazolyl]ethyl]thio]imidazole dihydrochloride (3b·2HCl): yield 70%; mp 289–292 °C from ethanol; ¹H-NMR (DMSO-*d*₆) δ 3.05 (t, *J* = 7.3 Hz, 2H, CH₂), 3.62 (t, *J* = 7.3 Hz, 2H, CH₂-S), 7.52 (d, *J* = 8.6 Hz, 2H, Ph-H), 7.54 (s, 1H, Im-5-H), 7.90 (d, *J* = 8.6 Hz, 2H, Ph-H), 8.08 (s, 1H, Ph-Im-5-H), 9.00 (s, 1H, Im-2-H). Anal. (C₁₄H₁₃ClN₄S·2HCl) C, H, N.

4(5)-(4-Nitrophenyl)-2-[[2-[4(5)-imidazolyl]ethyl]thio]imidazole dihydrochloride (3c·2HCl): yield 79%; mp 245–246 °C dec from ethanol; ¹H-NMR (DMSO-*d*₆) δ 2.88 (t, *J* = 7.4 Hz, 2H, CH₂), 3.33 (t, *J* = 7.4 Hz, 2H, CH₂-S), 6.90 (s, 1H, Im-5-H), 7.66 (s, 1H, Ph-Im-5-H), 7.95 (s, 1H, Im-2-H), 7.98 (d, *J* = 9.0 Hz, 2H, Ph-H), 8.21 (d, *J* = 9.0 Hz, 2H, Ph-H). Anal. (C₁₄H₁₃N₅O₂S·2HCl) C, H, N.

4(5)-(4-*n*-butoxyphenyl)-2-[[2-[4(5)-imidazolyl]ethyl]thio]imidazole dihydrochloride (3d·2HCl): yield 75%; mp 238–239 °C from ethanol/ethyl ether; ¹H-NMR (DMSO-*d*₆) δ 0.94 (t, *J* = 7.4 Hz, 3H, CH₃), 1.44 (m, 2H, CH₂), 1.70 (m, 2H, CH₂), 2.85 (t, *J* = 7.7 Hz, 2H, CH₂-Im), 3.25 (t, *J* = 7.7 Hz, 2H, CH₂S), 3.96 (t, *J* = 6.5 Hz, 2H, CH₂OPh), 6.86 (s, 1H, Im-5-H), 6.91 (d, *J* = 8.7 Hz, 2H, Ph-H), 7.45 (s, 1H, Ph-Im-5-H), 7.60 (s, 1H, Im-2-H), 7.63 (d, *J* = 8.7 Hz, 2H, Ph-H). Anal. (C₁₈H₂₂N₄OS·2HCl) C, H, N.

4(5)-(4-*n*-Propylphenyl)-2-[[2-[4(5)-imidazolyl]ethyl]thio]imidazole dihydrochloride (3e·2HCl): yield 80%; mp 235–237 °C from ethanol/water; ¹H-NMR (DMSO-*d*₆) δ 0.88 (t, *J* = 7.2 Hz, 3H, CH₃), 1.60 (m, 2H, CH₂), 2.58 (t, *J* = 7.2 Hz, 2H, CH₂Ph), 3.05 (t, *J* = 7.0 Hz, 2H, CH₂-Im), 3.74 (t, *J* = 7.0 Hz, 2H, CH₂S), 7.29 (d, *J* = 8.0 Hz, 2H, Ph-H), 7.58 (s, 1H, Ph-Im-5-H), 7.85 (d, *J* = 8.0 Hz, 2H, Ph-H), 8.13 (s, 1H, Ph-Im-5-H), 9.04 (s, 1H, Im-2-H). Anal. (C₁₇H₂₀N₄S·2HCl) C, H, N.

4(5)-[4-(Dimethylamino)phenyl]-2-[[2-[4(5)-imidazolyl]ethyl]thio]imidazole (3f): yield 61%; mp 127–129 °C from ethanol; ¹H-NMR (DMSO-*d*₆) δ 2.87 (t, *J* = 7.45 Hz, 2H, CH₂), 2.89 (s, 6H, CH₃), 3.24 (t, *J* = 7.5 Hz, 2H, CH₂S), 6.71 (d, *J* = 8.9 Hz, 2H, Ph-H), 6.92 (s, 1H, Im-5-H), 7.31 (s, 1H, Ph-Im-5-H), 7.53 (d, *J* = 8.9 Hz, 2H, Ph-H), 7.73 (s, 1H, Im-2-H). Anal. (as triplicate: C₁₆H₁₉N₅S·3C₆H₃N₃O₇) C, H, N.

4(5)-[4-(Phenylsulfonyl)oxy]phenyl]-2-[[2-[4(5)-imidazolyl]ethyl]thio]imidazole dihydrochloride (3g·2HCl): yield 90%; mp 197–198 °C from ethanol/ethyl ether; ¹H-NMR (DMSO-*d*₆) δ 2.85 (t, *J* = 7.4 Hz, 2H, CH₂), 3.27 (t, *J* = 7.4 Hz, 2H, CH₂S), 6.85 (s, 1H, Im-5-H), 6.98 (d, 2H, Ph-H), 7.56–7.87 (m, 9H, Ph-H + Im-H). Anal. (C₂₀H₁₈N₄O₃S₂·2HCl) C, H, N.

4(5)-(4-Carbamoylphenyl)-2-[[2-[4(5)-imidazolyl]ethyl]thio]imidazole dihydrochloride (3h·2HCl): yield 55%; mp 277–280 °C from ethanol/ethyl ether; ¹H-NMR (DMSO-*d*₆) δ 2.88 (t, *J* = 7.4 Hz, 2H, CH₂), 3.30 (t, *J* = 7.4 Hz, 2H, CH₂S), 6.94 (s, 1H, Im-5-H), 7.26 (bs, 1H, CONH₂), 7.74 (s, 1H, Ph-Im-5-H), 7.75 (s, 1H, Im-2-H), 7.79 (d, *J* = 8.2 Hz, 2H, Ph-H), 7.86 (d, *J* = 8.2 Hz, 2H, Ph-H), 7.91 (bs, 1H, CONH₂). Anal. (C₁₅H₁₅N₅OS·2HCl) C, H, N.

4(5)-(3-Bromophenyl)-2-[[2-[4(5)-imidazolyl]ethyl]thio]imidazole dihydrochloride (3i·2HCl): yield 89%; mp 277–278 °C from methanol/ethyl ether; ¹H-NMR (DMSO-*d*₆) δ 3.05 (t, *J* = 7.0 Hz, 2H, CH₂), 3.70 (t, *J* = 7.0 Hz, 2H, CH₂-S), 7.42 (t, *J* = 7.9 Hz, 1H, Ph-H), 7.53–7.58 (m, 2H, Im-5-H + Ph-H), 7.94 (d, *J* = 7.9 Hz, 1H, Ph-H), 8.18 (s, 1H, Ph-H), 8.20 (s, 1H, Ph-Im-5-H), 9.02 (s, 1H, Im-2-H). Anal. (C₁₄H₁₃N₄SBr·2HCl) C, H, N.

4(5)-(3-Nitrophenyl)-2-[[2-[4(5)-imidazolyl]ethyl]thio]imidazole (3j): yield 94%; mp 216–217 °C from ethanol/ethyl ether; ¹H-NMR (DMSO-*d*₆) δ 2.85 (t, *J* = 7.4 Hz, 2H, CH₂), 3.30 (t, *J* = 7.4 Hz, 2H, CH₂S), 6.84 (s, 1H, Im-5-H), 7.53 (s, 1H, Ph-Im-5-H), 7.63 (t, *J* = 7.9 Hz, 1H, Ph-H), 7.90 (s, 1H, Im-2-H), 8.02 (d, *J* = 7.9 Hz, 1H, Ph-H), 8.17 (d, *J* = 7.9 Hz, 1H, Ph-H), 8.54 (s, 1H, Ph-H). Anal. (C₁₄H₁₃N₅O₂S) C, H, N.

4(5)-(3-*n*-Propoxyphenyl)-2-[[2-[4(5)-imidazolyl]ethyl]thio]imidazole dihydrochloride (3k·2HCl): yield 95%; mp 230–233 °C from ethanol/ethyl ether; ¹H-NMR (DMSO-*d*₆) δ 0.99 (t, *J* = 7.4 Hz, 3H, CH₃), 1.73 (m, 2H, CH₂), 2.89 (t, *J* = 7.3 Hz, 2H, CH₂-Im), 3.29 (t, *J* = 7.3 Hz, 2H, CH₂S), 3.94 (t, *J* = 6.4 Hz, 2H, CH₂OPh), 6.74 (d, 1H, Ph-H), 6.96 (s, 1H, Im-5-H), 7.20–7.28 (m, 3H, Ph-H), 7.61 (s, 1H, Ph-Im-5-H), 7.83 (s, 1H, Im-2-H). Anal. (C₁₇H₂₀N₄OS·2HCl) C, H, N.

4(5)-(3-Carbamoylphenyl)-2-[[2-[4(5)-imidazolyl]ethyl]thio]imidazole dihydrochloride (3l·2HCl): yield 72%; mp 277–281 °C from ethanol/ethyl ether; ¹H-NMR (DMSO-*d*₆) δ 2.84 (t, *J* = 7.5 Hz, 2H, CH₂), 3.28 (t, *J* = 7.5 Hz, 2H, CH₂-S), 6.84 (s, 1H, Im-5-H), 7.32 (bs, 1H, CONH₂), 7.40 (t, *J* = 7.7 Hz, 1H, Ph-H), 7.55 (s, 1H, Ph-Im-5-H), 7.65 (s, 1H, Im-2-H), 7.68 (d, *J* = 7.7 Hz, 1H, Ph-H), 7.85 (d, *J* = 7.7 Hz, 1H, Ph-H), 7.94 (bs, 1H, CONH₂), 8.21 (s, 1H, Ph-H). Anal. (C₁₅H₁₅N₅OS·2HCl) C, H, N.

Ionization Constants and Partition Coefficients. The p*K*_a and log *P* values were determined by the pH-metric method²⁴ using a Sirius-PCA 101 instrument equipped with a semi-microcombined electrode, a precision dispenser, a six-way valve for distributing reagents and titrants (0.5 M HCl, 0.15 M KCl, 0.5 M NaOH, water-saturated octanol, methanol), a temperature probe, and a stirrer. Water and methanol contained 0.15 M KCl as an ionic strength adjuster. The weighted samples (0.5–4 mM) were added manually to the glass vessel while the titrant and all other reagents were supplied automatically. A circulating bath maintained the temperature of the sample solution at 25.0 ± 0.1 °C.

None of the compounds (with the exception of compound **3a**) was sufficiently water-soluble for normal aqueous titrations. Therefore the p*K*_a values were determined from 15–60 wt % methanol/water solutions and Yasuda–Shedlovsky extrapolation.⁴² log *P* values were calculated from octanol/water titrations and Bjerrum plots.²⁴ The approximate set of p*K*_a and log *P* constants so obtained were refined by a nonlinear least-squares procedure.⁴³

Pharmacology: H₃-Receptor Binding to Rat Brain Membranes. Binding affinities were measured in rat brain cortex membranes as previously described.⁴⁴ Membranes (0.5 mg of protein) of Wistar rat brain were incubated with the labeled ligand ([³H]NAMHA) in Tris-HCl, 50 mM, pH = 7.4, NaCl, 50 mM, EDTA, 1 mM. Incubation was ended by the addition of 4 mL of an ice-cold Tris-HCl/NaCl solution and rapid filtration on AAWP Millipore filters (pore diameter = 0.8 μm) under vacuum. Specific binding was defined as the binding inhibited by 1 μM thioperamide. Protein concentrations were measured by the Biorad method using bovine serum albumin as standard.

The p*K*_i values were calculated from the inhibition curves of the compounds tested vs 0.5 nM [³H]NAMHA, whose *K*_D measured independently was 0.62 nM.⁴⁴ Analysis of inhibition curves was performed with the software LIGAND⁴⁵ on the specific binding defined above. Both one-site and two-site models were tested, and the latter was chosen when a significant difference in fitting was observed by the *F*-test.⁴⁶ Standard error of the mean (SEM) was calculated from at least four independent experiments. Under these conditions, competitive binding assays with thioperamide gave a monophasic curve with p*K*_i = 8.49, nH = 1.01;⁴⁴ this result was in agreement with the *K*_i value reported by Arrang *et al.*,¹³ who employed [³H]-(*R*)-α-methylhistamine (*K*_i = 2.1 nM) as the labeled ligand. West *et al.* reported a biphasic inhibition of [³H]NAMHA binding for thioperamide, with two *K*_i values of 4.9 nM (*K*_{iA}) and 64 nM (*K*_{iB})⁴⁷ and a single *K*_i value of 16 nM vs [³H]-(*R*)-α-methylhistamine.⁴⁸ As these differences may be due to different ionic compositions of the solution,³⁰ we kept ionic composition constant during all experiments. In the competitive binding experiments, inhibitor concentrations up

to 10 μ M were tested, and therefore pK_i values lower than 6 could not be accurately calculated.

H₁, H₂, and H₃ Potency on Guinea Pig Peripheral Organs. Terminal ileum and atria, isolated from guinea pigs (350–550 g), were set up as previously described in detail.⁴⁹ Briefly, segments of the terminal ileum were suspended under 1 g load in a 10 mL tissue bath filled with Krebs Henseleit solution at 37 °C and bubbled with O₂ 95%:CO₂ 5%. Atria were set up under 0.5 g tension in a 20 mL organ bath containing Ringer-Locke solution at 32 °C and gassed with O₂ 95%:CO₂ 5%. Tissues were allowed to equilibrate for at least 60 min before the start of the experiments. Changes in mechanical activity of the tissues were recorded isometrically, and the variations in the atrial rate were detected by a cardiograph connected to the isometric transducer.

The H₃-receptor activity was studied on the tissue transmurally stimulated by means of two coaxial platinum electrodes (0.1 Hz, 1 ms, submax voltage). The H₃-antagonistic activity of the newly synthesized compounds, tested up to 10⁻⁶ M (30 min incubation), was determined on the concentration-dependent inhibition of twitch contractions induced by (*R*)- α -methylhistamine cumulatively administered (10⁻⁹–10⁻⁶ M).

To study H₁ activity in ileal smooth muscle or H₂ activity in atria, cumulative concentration–response curves to histamine (10⁻⁹–10⁻⁶ M) or to dimaprit (10⁻⁷–10⁻⁴ M) were respectively constructed in the presence and in the absence of the test compounds up to 10⁻⁶ M (30 min incubation).

The results were expressed as percentage of the maximum response induced by the agonist, and the data were reported as mean \pm SEM of 10–12 observations. EC₅₀ values and slopes of the regression line were calculated by analyzing the concentration–response curves by least-squares method. The antagonistic potency of the drugs tested were estimated by pA_2 determination calculated from Schild regression analysis. The statistical evaluation was performed using Student's *t*-test. *P* values < 0.05 were considered to be significant.

Data Analysis. PLS analysis was performed with the GOLPE program³⁷ running on an SGI Indigo2 R4400 200 MHz 64MB RAM workstation. The variables were autoscaled to unit variance before the calculation of the PLS model. The predictive power of the model was evaluated by cross-validation excluding one compound at a time (leave one out), and it was expressed by standard deviation of errors of predictions (SDEP) and Q^2 .³⁸ All of the cited 15 structural variables were initially included in the calculation of the PLS model. The values of these variables is given in Table 5 (Supporting Information). The second step of the analysis consisted in removing the noisy variables which decreased the predictive power of the model. This was achieved with the GOLPE procedure,³⁸ which evaluates the effect of each variable on the SDEP considering various combinations of variables and comparing their effect with that of “dummy” variables; the nine variables indicated in the work were selected for a two-latent-variable PLS model, with a combination/variables ratio of 5, 50% dummy variables, and retention of those with an uncertain effect.

Acknowledgment. Financial support from Italian MURST and CNR is gratefully acknowledged. B.T. and P.A.C. are grateful to the Swiss National Science Foundation for support.

Supporting Information Available: Structural data used in PLS analysis (1 page). Ordering information is given on any current masthead page.

References

- Arrang, J.-M.; Garbarg, M.; Schwartz, J. C. Auto-Inhibition of Brain Histamine Release Mediated by a Novel Class (H₃) of Histamine Receptor. *Nature* **1983**, *302*, 832–837.
- Schlicker, E.; Malinowska, B.; Kathmann, M.; Göthert, M. Modulation of Neurotransmitter Release via Histamine H₃ Heteroreceptors. *Fundam. Clin. Pharmacol.* **1994**, *8*, 128–137.
- Clapham, J.; Kilpatrick, G. J. Histamine H₃ Receptors Modulate the Release of [³H]-Acetylcholine from Slices of Rat Entorhinal Cortex: Evidence for the Possible Existence of H₃ Receptor Subtypes. *Br. J. Pharmacol.* **1992**, *107*, 919–923.
- Murakami, K.; Yokoyama, H.; Onodera, K.; Iinuma, K.; Watanabe, T. AQ-0145, a Newly Developed Histamine H₃ Antagonist, Decreased Seizure Susceptibility of Electrically Induced Convulsions in Mice. *Methods Find. Exp. Clin. Pharmacol.* **1995**, *17* (Suppl. C), 70–73.
- Yokoyama, H.; Iinuma, K. Histamine and seizures - Implications for the Treatment of Epilepsy. *CNS Drugs* **1996**, *5*, 321–330.
- Timmerman, H. Pharmacotherapy of Vertigo: Any News to be Expected? *Acta Oto-Laryngol., Suppl.* **1994**, *513*, 28–32.
- Prast, H.; Argyriou, H.; Philippu, A. Histaminergic Neurons Facilitate Social Memory in Rats. *Brain Res.* **1996**, *734*, 316–318.
- Miyazaki, S.; Imiazumi, M.; Onodera, K. Effects of Thioperamide, a Histamine H₃-Receptor Antagonist, on a Scopolamine-Induced Learning Deficit Using an Elevated Plus-Maze Test in Mice. *Life Sci.* **1995**, *57*, 2137–2144.
- Sakata, T. Histamine Receptor and its Regulation of Energy Metabolism. *Obes. Res.* **1995**, *3* (Suppl. 4), S541–S548.
- Leurs, R.; Vollinga, R. C.; Timmerman, H. The Medicinal Chemistry and Therapeutic Potentials of Ligands of the Histamine H₃ Receptor. *Prog. Drug Res.* **1995**, *45*, 107–165.
- Ganellin, C. R.; Fkyerat, A.; Hosseini, S. K.; Khalaf, Y. S.; Piripitsi, A.; Tertiuk, W.; Arrang, J. M.; Garbarg, M.; Ligneau, X.; Schwartz, J. C. Structure-Activity Studies with Histamine H₃-Receptor Ligands. *J. Pharm. Belg.* **1995**, *50*, 179–187.
- Plazzi, P. V.; Mor, M.; Bordi, F.; Silva, C.; Caretta, A.; Ballabeni, V.; Impicciatore, M.; Vitali, T. Ligands of the Histamine H₃-Receptor: New Potent Antagonists of the 2-Thioimidazole Type. *Il Farmaco*, in press.
- Arrang, J.-M.; Garbarg, M.; Lancelot, J. C.; Lecomte, J. M.; Pollard, H.; Robba, M.; Schunack, W.; Schwartz, J. C. Highly Potent and Selective Ligands for Histamine H₃-Receptors. *Nature* **1987**, *327*, 117–123.
- Van der Goot, H.; Schepers, M. J. P.; Sterk, G. J.; Timmerman, H. Isothiourea Analogues of Histamine as Potent Agonists or Antagonists of the Histamine H₃-Receptor. *Eur. J. Med. Chem.* **1992**, *27*, 511–517.
- Jansen, F. P.; Wu, T. S.; Voss, H.-P.; Steinbusch, H. W. M.; Vollinga, R. C.; Rademaker, B.; Bast, A.; Timmerman, H. Characterization of the Binding of the First Selective Radiolabelled Histamine H₃-Receptor Antagonist, [¹²⁵I]iodophenpropit, to Rat Brain. *Br. J. Pharmacol.* **1994**, *113*, 355–362.
- Ligneau, X.; Garbarg, M.; Vizuete, M. L.; Diaz, J.; Purand, K.; Stark, H.; Schunack, W.; Schwartz, J.-C. [¹²⁵I]iodoproxyfan, a new Antagonist to Label and Visualize Cerebral Histamine H₃ Receptors. *J. Pharmacol. Exp. Ther.* **1994**, *271*, 452–459.
- Ganellin, C. R.; Hosseini, S. K.; Khalaf, Y. S.; Tertiuk, W.; Arrang, J. M.; Garbarg, M.; Ligneau, X.; Schwartz, J. C. Design of Potent Non-Thiourea H₃-Receptor Histamine Antagonists. *J. Med. Chem.* **1995**, *38*, 3342–3350.
- Plazzi, P. V.; Bordi, F.; Mor, M.; Silva, C.; Morini, G.; Caretta, A.; Barocelli, E.; Vitali, T. Heteroarylthioethyl- and Heteroarylthioethylimidazoles. Synthesis and H₃-Receptor Affinity. *Eur. J. Med. Chem.* **1995**, *30*, 881–889.
- Clitherow, J. W.; Beswick, P.; Irving, W. J.; Scopes, D. I. C.; Barnes, J. C.; Clapham, J.; Brown, J. D.; Evans, D. J.; Hayes, A. G. Novel 1, 2, 4-Oxadiazoles as Potent and selective Histamine H₃ Receptor Antagonists. *Bioorg. Med. Chem. Lett.* **1996**, *6*, 833–838.
- Plazzi, P. V.; Mor, M.; Silva, C.; Bordi, F.; Morini, G.; Crivori, P.; Caretta, A. Rat Protein Binding and Cerebral Phospholipid Affinity of the H₃-Receptor Antagonist Thioperamide. *J. Pharm. Pharmacol.* **1996**, *48*, 712–717.
- Bordi, F.; Mor, M.; Morini, G.; Plazzi, P. V.; Silva, C.; Vitali, T.; Caretta, A. QSAR Study on H₃-Receptor Affinity of Benzothiazole Derivatives of Thioperamide. *Il Farmaco* **1994**, *49*, 153–166.
- Barocelli, E.; Ballabeni, V.; Chiavarini, M.; Caretta, A.; Mor, M.; Silva, C.; Impicciatore, M. Structural Analogues of Thioperamide: Pharmacological Evaluation of New Benzothiazole Derivatives at Peripheral Histamine Subtypes in Guinea-pigs. *Pharm. Sci.* **1995**, *1*, 177–180.
- Barocelli, E.; Ballabeni, V.; Caretta, A.; Chiavarini, M.; Bordi, F.; Mor, M.; Impicciatore, M. Functional Studies of New Imidazole H₃-Antagonists on Guinea-pig Isolated Preparation. *Pharm. Sci.* **1995**, *1*, 383–386.
- Avdeef, A. pH-Metric log P. Part 1. Difference plots for Determining Ion-Pair Octanol-Water Partition Coefficients of Multiprotic Substances. *Quant. Struct.-Act. Relat.* **1992**, *11*, 510–517.
- Baroni, M.; Clementi, S.; Cruciani, G.; Kettaneh-Wold, N.; Wold, S. D-Optimal Designs in QSAR. *Quant. Struct.-Act. Relat.* **1993**, *12*, 225–231.
- Skagerberg, B.; Bonelli, D.; Clementi, S.; Cruciani, G.; Ebert, C. Principal Properties for Aromatic Substituents. A Multivariate Approach for Design in QSAR. *Quant. Struct.-Act. Relat.* **1989**, *8*, 32–38.
- Box, G. E. P.; Hunter, W. G.; Hunter, J. S. *Statistics for Experimenters*; Wiley: New York, 1978; p 306.
- DESDOP v. 2.0; MIA srl; Perugia, Italy.

- (29) Hansch, C.; Leo, A.; Hoekman, D. *Exploring QSAR - Hydrophobic, Electronic, and Steric Constants*; American Chemical Society: Washington, DC, 1995.
- (30) Clark, E. A.; Hill, S. J. Differential Effect of Sodium Ions and Guanine Nucleotides on the Binding of Thioperamide and Clobenpropit to Histamine H₃-Receptors in Rat Cerebral Cortical Membranes. *Br. J. Pharmacol.* **1995**, *114*, 357–362.
- (31) Schlicker, E.; Kathmann, M.; Reidemeister, S.; Stark, H.; Schunack, W. Novel Histamine H₃ Receptor Antagonists: Affinities in an H₃ Receptor Binding Assay and Potencies in Two Functional H₃ Receptor Models. *Br. J. Pharmacol.* **1994**, *112*, 1043–1048.
- (32) Schlicker, E.; Kathmann, M.; Bitschnau, H.; Marr, I.; Reidemeister, S.; Stark, H.; Schunack, W. Potencies of Antagonists Chemically Related to Iodoproxyfan at Histamine H₃ Receptors in Mouse Brain Cortex and Guinea-Pig Ileum: Evidence for H₃ Receptor Heterogeneity? *Naunyn-Schmiedeberg's Arch. Pharmacol.* **1996**, *353*, 482–488.
- (33) Leurs, R.; Kathmann, M.; Vollinga, R. C.; Menge, W. M. P. B.; Schlicker, E.; Timmerman, H. Histamine Homologues Discriminating between Two Functional H₃ Receptor Assays. Evidence for H₃ Receptor Heterogeneity? *J. Pharmacol. Exp. Ther.* **1996**, *276*, 1009–1015.
- (34) Norrington, F. E.; Hyde, R. M.; Williams, S. G.; Wootton, R. Physicochemical-Activity Relations in Practice. 1. A Rational Self-Consistent Data Bank. *J. Med. Chem.* **1975**, *18*, 604–607.
- (35) Austel, V.; Kutter, E.; Kalbfleisch, W. A New Easily Accessible Steric Parameter for Structure-Activity Relationships. *Arzneim. Forsch.* **1979**, *29*, 585–587.
- (36) Topliss, J. G.; Edwards, R. P. Chance Factors in Studies of Quantitative Structure-Activity Relationships. *J. Med. Chem.* **1979**, *22*, 1238–1244.
- (37) GOLPE v. 3.0.1, MIA srl, Perugia, Italy.
- (38) Baroni, M.; Costantino, G.; Cruciani, G.; Riganelli, D.; Valigi, R.; Clementi, S. Generating Optimal PLS Estimations (GOLPE): An Advanced Chemometric Tool for Handling 3D-QSAR Problems. *Quant. Struct.-Act. Relat.* **1993**, *12*, 9–20.
- (39) Norris, T.; McKee, R. L. 2-Guanidino-4(5)-*p*-chlorophenylimidazoles. *J. Am. Chem. Soc.* **1955**, *77*, 1056.
- (40) Grant, R. L.; Pyman, F. L. The Nitro- and Amino-derivatives of 4-Phenylglyoxaline. *J. Chem. Soc.* **1921**, *119*, 1893–1903.
- (41) Snyder, H. R.; Elston, T. Polyphosphoric Acid as a Reagent in Organic Chemistry. VI. The Hydrolysis of Nitriles to Amides. *J. Am. Chem. Soc.* **1954**, *76*, 3039–3040.
- (42) Avdeef, A.; Comer, J. E. A.; Thomson, S. J. pH-Metric log P. 3. Glass Electrode Calibration in Methanol-Water, Applied to pK_a Determination of Water-Insoluble Substances. *Anal. Chem.* **1993**, *65*, 42–49.
- (43) Avdeef, A. pH-Metric log P. II: Refinement of Partition Coefficients and Ionization Constants of Multiprotic Substances. *J. Pharm. Sci.* **1993**, *82*, 1–8.
- (44) Bordi, F.; Mor, M.; Plazzi, P. V.; Silva, C.; Morini, G.; Caretta, A.; Barocelli, E.; Impicciatore, M. Synthesis and Binding Assays of H₃-Receptor Ligands. *Il Farmaco* **1992**, *47*, 1343–1365.
- (45) Munson, P. J.; Rodbard, D. LIGAND: A Versatile Computerized Approach for Characterization of Ligand-Binding Systems. *Anal. Biochem.* **1980**, *107*, 220–239.
- (46) Sprague, E. D.; Larrabee, C. E., Jr.; Halsall, H. B. Statistical Evaluation of Alternative Models: Application to Ligand-Protein Binding. *Anal. Biochem.* **1980**, *101*, 175–181.
- (47) West, R. E., Jr.; Zweig, A.; Shih, N.-Y.; Siegel, M. I.; Egan, R. W.; Clark, M. A. Identification of Two H₃-Histamine Receptor Subtypes. *Mol. Pharmacol.* **1990**, *38*, 610–613.
- (48) West, R. E., Jr.; Zweig, A.; Granzow, R. T.; Siegel, M. I.; Egan, R. W. Biexponential Kinetics of (R)- α -[³H]Methylhistamine Binding to the Rat Brain H₃ Histamine Receptor. *J. Neurochem.* **1990**, *55*, 1612–1616.
- (49) Barocelli, E.; Ballabeni, V.; Caretta, A.; Bordi, F.; Silva, C.; Morini, G.; Impicciatore, M. Pharmacological Profile of New Thioperamide Derivatives at Histamine Peripheral H₁-, H₂-, H₃-Receptors in Guinea-Pig. *Agents Actions* **1993**, *38*, 158–164.

JM970070P